

RESEARCH ARTICLE

# Copper Nanoparticles and Copper Sulphate Induced Cytotoxicity in Hepatocyte Primary Cultures of *Epinephelus coioides*

Tao Wang, Xiaoyan Chen, Xiaohua Long\*, Zhaopu Liu, Shaohua Yan

Jiangsu Provincial Key Laboratory of Marine Biology, College of Resources and Environmental Sciences, Nanjing Agricultural University, Nanjing, 210095, P.R. China

\* [longxiaohua@njau.edu.cn](mailto:longxiaohua@njau.edu.cn)



OPEN ACCESS

**Citation:** Wang T, Chen X, Long X, Liu Z, Yan S (2016) Copper Nanoparticles and Copper Sulphate Induced Cytotoxicity in Hepatocyte Primary Cultures of *Epinephelus coioides*. PLoS ONE 11(2): e0149484. doi:10.1371/journal.pone.0149484

**Editor:** Ferenc Gallyas, Jr., University of Pecs Medical School, HUNGARY

**Received:** November 2, 2015

**Accepted:** February 2, 2016

**Published:** February 18, 2016

**Copyright:** © 2016 Wang et al. This is an open access article distributed under the terms of the [Creative Commons Attribution License](https://creativecommons.org/licenses/by/4.0/), which permits unrestricted use, distribution, and reproduction in any medium, provided the original author and source are credited.

**Data Availability Statement:** All data are available in the paper; there are no files with supporting information.

**Funding:** The authors are grateful for the financial support of the National Key Projects of Scientific and Technical Support Programs funded by the Ministry of Science and Technology of China (No. 2011BAD13B09).

**Competing Interests:** The authors have declared that no competing interests exist.

## Abstract

Copper nanoparticles (Cu-NPs) were widely used in various industrial and commercial applications. The aim of this study was to analyze the cytotoxicity of Cu-NPs on primary hepatocytes of *E. coioides* compared with copper sulphate (CuSO<sub>4</sub>). Cultured cells were exposed to 0 or 2.4 mg Cu L<sup>-1</sup> as CuSO<sub>4</sub> or Cu-NPs for 24-h. Results showed either form of Cu caused a dramatic loss in cell viability, more so in the CuSO<sub>4</sub> than Cu-NPs treatment. Compared to control, either CuSO<sub>4</sub> or Cu-NPs significantly increased reactive oxygen species (ROS) and malondialdehyde (MDA) concentration in hepatocytes by overwhelming total superoxide dismutase (T-SOD) activity, catalase (CAT) activity and glutathione (GSH) concentration. In addition, the antioxidative-related genes [*SOD (Cu/Zn)*, *SOD (Mn)*, *CAT*, *GPx4*] were also down-regulated. The apoptosis and necrosis percentage was significantly higher after the CuSO<sub>4</sub> or Cu-NPs treatment than the control. The apoptosis was induced by the increased cytochrome c concentration in the cytosol and elevated caspase-3, caspase-8 and caspase-9 activities. Additionally, the apoptosis-related genes (*p53*, *p38β* and *TNF-α*) and protein (p53 protein) were up-regulated after the CuSO<sub>4</sub> or Cu-NPs treatment, with CuSO<sub>4</sub> exposure having a greater effect than Cu-NPs. In conclusion, Cu-NPs had similar types of toxic effects as CuSO<sub>4</sub> on primary hepatocytes of *E. coioides*, but toxicity of CuSO<sub>4</sub> was more severe than that of Cu-NPs.

## Introduction

Owing to their unique chemical and physical properties that emerge at the nanoscale, engineered copper nanoparticles (Cu-NPs) are found in a broad range of industrial and scientific applications as well as in consumer products [1,2]. They are also used in environmental remediation for the removal of organic pollutants or as a versatile biocide [3]. Even though true global production volumes of Cu-NPs are presently unknown, their broad use is highly likely going to result in a release into aquatic systems and the contact with non-target, aquatic organisms [2,4]. In the last decade, concerns were raised about the effects of metal nanoparticles on fish, including sublethal effects of nanoparticles on the different body systems of fish [5–7]. However,

most studies to understand the toxicity of Cu-NPs were performed in whole fish. To our knowledge, the understanding of Cu-NPs toxicity to fish cells is limited, and no study reported toxicity of Cu-NPs on primary hepatocytes of *E.coioides*.

In aquaculture production, CuSO<sub>4</sub> is used to control diseases and algae [8]. Toxicity of CuSO<sub>4</sub> to fishes is relatively well known, including tissue injuries [9,10], osmoregulatory disturbances [11,12], and oxidative stress [9,13,14]. However, so far, no study has investigated possible mechanisms of CuSO<sub>4</sub> toxicity on hepatocytes of *E.coioides*.

*E.coioides*, a protogynous hermaphroditic fish, is a major farmed marine fish in China and Southeast Asian counties [15]. Currently, *E.coioides* were mainly cultured in floating net cages and earthen ponds in the natural environment that can easily be affected by environmental pollution [16]. The discharge of Cu-NPs or CuSO<sub>4</sub> in the aquatic environment is inevitable [10]. A deeper understanding of the toxic effects of Cu-NPs or CuSO<sub>4</sub> to *E.coioides* might help in development of guidelines to fish culture, and also to human food safety.

Previously, we studied the toxic effects of Cu-NPs on juvenile *E.coioides* (cultured in seawater) compared with CuSO<sub>4</sub>, and found that Cu from CuSO<sub>4</sub> was more toxic to liver than the equal concentration of Cu-NPs [7]. In the present study, we investigated the toxic effects of Cu-NPs and CuSO<sub>4</sub> on hepatocyte primary cultures of *E.coioides*. The aims of this study were to find whether liver toxicity *in vivo* can be replicated in hepatocyte cultures, and to explore the mechanisms of Cu-NPs and CuSO<sub>4</sub> toxicity to *E.coioides* at the cellular level.

## Materials and Methods

### Ethics statement

All experimental protocols were approved by the Institutional Animal Care and Use Committee of Nanjing Agricultural University (Nanjing, China). To collect tissues, fish were euthanized (MS-222 at 10 mg L<sup>-1</sup>) according to the Guide for the Care and Use of Laboratory Animals in China.

### Nanoparticle characterization

The Cu-NPs were purchased from Shanghai Aladdin Co., Ltd. China, with an average particle diameter of 20±10nm and 99.9% purity (manufacturer's specification). Cu-NPs suspension containing 1.0 g Cu L<sup>-1</sup> was prepared by dispersing nanoparticles in ultrapure water (Millipore, ion free and unbuffered), sonicated for 30 min and stirred for 1 h at room temperature to increase dispersion before use [10,17]. Copper ion stock solution (1.0 g Cu L<sup>-1</sup>) was prepared by dissolving 3.929 g CuSO<sub>4</sub>·5H<sub>2</sub>O in 1 L of ultrapure water.

As in our previous study [18], the particle size was characterized using transmission electron microscopy (TEM, JEOL JEM-2100, Japan) and nanoparticle tracking analysis (NTA, NanoSight LM10). For TEM analysis, Cu-NPs were diluted in ultrapure water (Millipore, ion free and unbuffered) and sonicated 30 min to keep the particles in solution and avoid aggregation [19,20]. The primary range of particle sizes was determined from micrographs through analysis of 50 NPs selected randomly. Additionally, particle size distribution in the cell culture medium [DMEM/F12 medium in the presence of 15% (v/v) serum, 100 IU mL<sup>-1</sup> penicillin and 100 IU mL<sup>-1</sup> streptomycin] were measured by NTA in 20 mg Cu L<sup>-1</sup> to give sufficient particle tracks (>100 tracks per sample) [21].

### Primary hepatocytes from *E.coioides*

Hepatocytes culture was carried out as previously described [22]. Briefly, liver was obtained from healthy juvenile *E.coioides* and washed several times in ice-cold phosphate-buffered saline

(PBS) containing 100 IU mL<sup>-1</sup> penicillin and 100 IU mL<sup>-1</sup> streptomycin (Sigma Chemical Company, St. Louis, MO), then the liver was cut into small pieces (about 1 mm), placed into 25-cm<sup>2</sup> tissue culture flasks and cultured in fresh Dulbecco modified Eagle F-12 medium (DMEM) in the presence of 15% (v/v) serum and 100 IU mL<sup>-1</sup> of each penicillin and streptomycin at 28°C in an incubator with 5% (v/v) CO<sub>2</sub>; the medium was replaced every 3 days. After 1 week, cells grew out of the explants, and the explants were removed. Upon reaching confluency, cells were harvested in 0.25% (w/v) trypsin-EDTA, suspended at a density of 1×10<sup>6</sup> cells mL<sup>-1</sup>, and counted using 0.4% (w/v) trypan-blue and an inverted microscope (TE 2000 Microscope, Nikon, Japan) to confirm that cell viability exceeded 90% for subsequent experimentation.

## Hepatocyte sub-culturing and treatment

Cell suspensions were seeded onto 6-well or 96-well plates depending on the experiments, incubated at 28°C with 5% (v/v) CO<sub>2</sub>. The medium (as above) was replaced every 3 d until 80–90% confluent, at which time cells were transferred into culture medium containing 0 or 2.4 mg Cu L<sup>-1</sup> as CuSO<sub>4</sub> or Cu-NPs for 24 h. Three replicates were performed for each treatment. The concentration of 2.4 mg Cu L<sup>-1</sup> Cu was chosen because it represents half of 24-h LC<sub>50</sub> concentration of Cu-NPs for juvenile *E.coioides*. In addition, this concentration reflects point-source environmental pollution (e.g. some areas with intensive agricultural and mining activities, manufacturing industries and municipal waste depositions) [23]. After exposure, cells were harvested in 0.25% (w/v) trypsin-EDTA at room temperature for cellular biochemical assays.

## Cytotoxicity assays

Cytotoxic responses of *E.coioides* hepatocytes in CuSO<sub>4</sub> or Cu-NPs were measured by the MTT [3-(4,5-dimethyl-2-thiazolyl)-2,5-diphenyl-2-H-tetrazoliumbromide] and LDH (lactate dehydrogenase) leakage assays.

## MTT assay

Viability of hepatocytes after exposure to CuSO<sub>4</sub> or Cu-NPs was assessed by MTT assay as described by Ahamed et al. [24] with some modifications. The MTT assay assesses the mitochondrial function by measuring ability of viable cells to reduce MTT into blue formazan product. In brief, suspension of primary cell cultures (1×10<sup>5</sup> cells mL<sup>-1</sup>) was seeded in 6-well plates, incubated at 28 °C with 5% (v/v) CO<sub>2</sub> until 80–90% confluent, then exposed to control (0) or 2.4 mg Cu L<sup>-1</sup> as CuSO<sub>4</sub> or Cu-NPs for 24 h. At the end of exposure, solution of MTT (0.5 mg mL<sup>-1</sup>) was added and cells were incubated under normal culture conditions for 4 h. The resulting formazan crystals were dissolved in isopropanol acidified with 0.04 N HCl. Further, a 200-μL aliquot of supernatant was transferred to clean wells of a 96-well plate, and absorbance was measured at 570 nm by using a microplate reader (Bio-Rad, USA).

## LDH leakage assay

The assay was carried out using an LDH cytotoxicity assay kit (Beyotime Institute of Biotechnology, Haimen, Jiangsu, China). In brief, 1×10<sup>4</sup> cells/well were seeded in 96-well plates at a final volume of 200μL culture medium/well, incubated at 28 °C with 5% (v/v) CO<sub>2</sub> until 80–90% confluent, then exposed to control (0) or 2.4 mg Cu L<sup>-1</sup> as CuSO<sub>4</sub> or Cu-NPs for 24 h. At the end of treatment, LDH concentration in the media and the cells was quantified and

compared to the control values using a microplate reader (Bio-Rad, USA) at 340 nm according to the manufacturer's protocol.

### Reactive oxygen species (ROS) generation

ROS generation was measured using 2,7-dichlorofluoresceindiacetate (DCFH-DA) as described by Xu et al. [22] with some modifications. In brief, 500  $\mu\text{L}$  of hepatocytes ( $1 \times 10^7$  cells  $\text{mL}^{-1}$ ) were collected after  $\text{CuSO}_4$  or Cu-NPs exposure, then incubated in PBS buffer with  $10 \mu\text{mol L}^{-1}$  DCFH-DA at  $28^\circ\text{C}$  in the dark for 1 h, and the fluorescence intensity was measured at 485 nm excitation and 520 nm emission using a microplate reader (Bio-Rad, USA). The values were expressed as a percent of fluorescence intensity relative to control wells.

### Oxidative stress detection

After  $\text{CuSO}_4$  or Cu-NPs exposure, hepatocytes ( $1 \times 10^7$  cells  $\text{mL}^{-1}$ ) were collected, homogenized with a glass grinder, and centrifuged at  $800 \times g$  at  $4^\circ\text{C}$  for 10 min; the supernatant was used for oxidative stress analysis. Activities of catalase (CAT) and total superoxide dismutase (T-SOD) and concentrations of malondialdehyde (MDA) and glutathione (GSH) were detected using kits (Nanjing Jiancheng Bioengineering Research Institute, Nanjing, China) according to the manufacturer's instructions [7,22]. CAT activity was determined based on ammonium molybdate spectrophotometry. T-SOD activity was determined based on the WST-1 (water-soluble tetrazolium salt) method. The MDA concentration was determined via modified NBT (nitroblue tetrazolium) method [25]. GSH was determined based on the recycling reaction of GSH with DNTB (5,5'-dithio-(2-nitrobenzoic acid)) in the presence of excess glutathione reductase. The protein content was determined using the Bradford's method [26].

### Cell apoptosis and necrosis detection

According to Cui et al. [27], apoptosis and necrosis were quantified by Annexin V-FITC/PI apoptosis detection kit (Nanjing Key-gen Biotech. Co., Ltd. Nanjing, China). Briefly, cells were collected after  $\text{CuSO}_4$  or Cu-NPs exposure ( $5 \times 10^5$  cells  $\text{mL}^{-1}$ ) and washed with PBS. The cells were resuspended in the Annexin V-FITC staining reagent and fixed at  $28^\circ\text{C}$  for 15 min. Then the cells were washed and resuspended in the PI staining reagent. Staining was stable at  $4^\circ\text{C}$  for 30 min [27,28]. Samples were then analyzed by flow cytometry (Becton Dickinson, San Jose, CA).

### Nuclear ultrastructure observation

The collected cells ( $1 \times 10^7$  cells  $\text{mL}^{-1}$ ) were fixed with PBS containing 2.5% (v/v) glutaraldehyde followed by treatment with PBS containing 1% (v/v) osmium tetroxide ( $\text{OsO}_4$ ). The samples were dehydrated in a graded series of alcohol (30%, 50%, 70%, 80%, 90%, 95% and 100%, v/v) for 15 min at each concentration, embedded in epoxy resin Epon812, and sectioned (60 nm) using an ultra-microtome (LKB Nova, Bromma, Sweden). Ultrathin sections were stained with 4% (w/v) uranyl acetate, as well as lead citrate, and observed using an H-7650 transmission electron microscope (Hitachi High-Technologies Co., Japan).

### Cytochrome c concentration

After exposure, hepatocytes ( $1 \times 10^7$  cells  $\text{mL}^{-1}$ ) were harvested and centrifuged at  $800 \times g$  at  $4^\circ\text{C}$  for 10 min; the pellets were used for cytochrome c detection. According to Xu et al. [22], cytochrome c was analyzed by isolation of mitochondrial and cytosolic proteins using mitochondria/cytosol fractionation kit (Nanjing Jiancheng Bioengineering Research Institute, Nanjing, China). The details were described in our previous study [18]. Cytochrome c concentration was

measured using enzyme-linked immunosorbent kit (ELISA) (Nanjing Jiancheng Bioengineering Research Institute, Nanjing, China), according to the manufacturer's protocol, with the optical density (OD) of each well determined using an ELISA reader at 450 nm.

### Caspases

Activities of caspase-3, caspase-8 and caspase-9 were measured using commercial kits (Nanjing Jiancheng Bioengineering Research Institute, Nanjing, China) according to the method of Jia et al. [14]. Briefly, cells ( $1 \times 10^7$  cells  $\text{mL}^{-1}$ ) were collected by centrifugation ( $800 \times g$ ,  $4^\circ\text{C}$ , 10 min) after  $\text{CuSO}_4$  or Cu-NPs exposure and washed twice with PBS, and then homogenized in lysis buffer. The lysates were centrifuged at  $10,000 \times g$  at  $4^\circ\text{C}$  for 15 min, and the supernatants were incubated in the dark at  $28^\circ\text{C}$  for 4 h with  $5 \mu\text{L}$  ( $0.2 \text{ mM}$ ) of each Ac-DEVD-pNA (acetyl-Asp-Glu-Val-Asp p-nitroanilide), Ac-IETD-pNA (acetyl-Ile-Glu-Thr-Asp p-nitroanilide), and Ac-LEHD-pNA (acetyl-Leu-Glu-His-Asp p-nitroanilide) as the substrates for caspase-3, caspase-8 and caspase-9, respectively. The absorbance at 405 nm was read using a microplate reader (Bio-Rad, USA). The reaction with lysis buffer instead of test samples was used as the negative control. The caspase-3, caspase-8 and caspase-9 activities were calculated as  $\text{OD}(\text{treatment})/\text{OD}(\text{negative control})$ .

### Gene expression and protein abundance

**Gene expression.** After exposure, cells ( $1 \times 10^7$  cells  $\text{mL}^{-1}$ ) were harvested and centrifuged at  $800 \times g$  at  $4^\circ\text{C}$  for 10 min and washed twice with PBS; the pellets were used for gene expression and protein abundance analyses. Total RNA was extracted from hepatocytes using RNAiso reagent (Takara Co. Ltd, Japan) according to the manufacturer's instructions. Concentration of extracted RNA was determined using a Nanodrop1000 (Thermo Fisher Scientific, USA), and the integrity of RNA was visualized on 1.0% (w/v) formaldehyde denaturing agarose gel.

The cDNA was synthesised using PrimeScript RT-PCR Kit (Takara Co. Ltd, Japan) according to the manufacturer's instructions. To adjust for the quantity of input cDNA, the house-keeping gene  $\beta$ -actin was used as an internal control. Primers (Table 1) for RT-PCR were designed with reference to the known sequences of *E.coioides* in GenBank.

RT-PCR was performed by SYBR Premix EX Taq (Takara Co. Ltd, Japan) using an ABI 7500 Real Time PCR System (Applied Biosystems, Foster City, CA, USA). An aliquot of  $2.0 \mu\text{L}$  of template cDNA was added to the final volume of  $20 \mu\text{L}$  of reaction mixture. An RT-PCR protocol consisted of initial denaturation at  $95^\circ\text{C}$  for 30 s, followed by 40 cycles of  $95^\circ\text{C}$  for 3 s each, and annealing at  $60^\circ\text{C}$  for 34 s. The dissociation stage included  $95^\circ\text{C}$  for 15 s,  $60^\circ\text{C}$  for 1 min and  $95^\circ\text{C}$  for 15 s. We calculated the relative quantity of the target gene transcripts with a chosen reference gene transcript ( $\beta$ -actin) using the  $2^{-\Delta\Delta\text{CT}}$  method [29].

**Table 1. Nucleotide sequences of the primers used to assay gene expression by real-time PCR.**

Target gene	GenBank accession no.	Forward (5'-3')	Reverse (5'-3')
$\beta$ -actin	AY510710	GGCTACTCCTTACCACCACA	GGGCAACGGAACCTCTCAT
SOD (Cu/Zn)	AY735008	TGGAGAGACCAGTGGGACCGT	GCAGTCACATTTCCCAGGTC
SOD (Mn)	AY735007	CGGCTCCTCCAGAAGATGA	CTCCCAGTTGATGACATTCCAGAT
CAT	AY735009	GGCGTTTGGTTACTTTGAGGT	AGAAGCGGACAGCAATAGGTG
GPx4	HQ441085	ACATCCTTGCCCTCCCTTC	CCCGTTCACATCGTCCTTA
p53	HM622380	CGCAACAGGCTTCAATCGT	GAAGCATCAGAGGCGAAGA
p38 $\beta$	JN408833	CAGAGACCTCAAGCCAAGTAATGT	TCGATGTAGTCAGTCCAGGAAAG
TNF- $\alpha$	FJ009049	CCTGGTGATGTGGAGATG	GTCCGACTTGATTAGTGCTT

doi:10.1371/journal.pone.0149484.t001

**Protein abundance.** Western blot was used for p53 protein abundance analysis according to the method of Ahamed et al. [24] with some modifications. Cells were lysed in RIPA buffer [1× TBS(0.5 M Tris-HCl and 1.5 M NaCl) pH 7.4, 1% (v/v) NP-40, 0.5% (w/v) sodium deoxycholate, 0.1% (w/v) SDS, 0.004% (w/v) sodium azide] supplemented with DL-dithiothreitol (DTT) and proteinase inhibitors. The cellular lysates were clarified by centrifugation at 15,000× g at 4°C for 10 min. Aliquots of the protein extracts were resolved on SDS-PAGE gels, and transferred to nitrocellulose (NC) membranes. Membranes were blocked with 5%(w/v) non-fat dry milk in PBS buffer containing 0.05% (v/v) Tween20, and incubated with rabbit anti-*E.coioides* p53 and β-actin monoclonal antibodies (1: 800 dilution) (Abcam, UK) [30]. Specific protein signals were detected by incubating membranes with peroxidase-conjugated anti-rabbit antibodies (1: 2000 dilution) and visualizing with a chemiluminescence reagent (Pierce Biotechnology, Rockford, IL).

## Statistical analysis

Data were analyzed by one-way analysis of variance (ANOVA) using SPASS (19.0). Tukeys' test was used to compare differences among treatments ( $p < 0.05$ ). Data were tested for normality using the Kolmogorov-Smirnov test and for homogeneity of variances by Levene's test; when necessary, the data were log-transformed [31]. All data were expressed as means ± standard deviation (SD).

## Results

### Characteristics of Cu-NPs used in this study

The Cu-NPs observed by TEM were spherical in shape and aggregated (Fig 1A), with a mean primary particle diameter of  $80 \pm 32$  nm (mean ±SD, n = 50) (Fig 1B). Using NTA, the average diameter of Cu-NPs in cell culture medium was determined to be  $100 \pm 35$  nm.

### Cytotoxicity

Fig 2 represents cytotoxicity induced by Cu from  $\text{CuSO}_4$  or Cu-NPs in the primary hepatocytes of *E.coioides*. After exposure, cell viability of hepatocytes significantly decreased compared to control ( $p < 0.05$ ), but more so in the  $\text{CuSO}_4$  than Cu-NPs treatment. However, the  $\text{CuSO}_4$  treatment resulted in a significantly higher percentage of LDH leakage than Cu-NPs ( $p < 0.05$ ).

### ROS production

We measured ROS production using the fluorescent dye DCF-DA (Fig 3A). Compared to control, exposure to either  $\text{CuSO}_4$  or Cu-NPs significantly increased ROS generation ( $p < 0.05$ ),

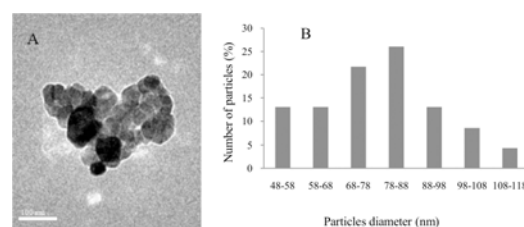


**Fig 1. Characteristics of Cu-NPs used in this study.** Transmission electron microscopy (TEM) image, scale bar = 100 nm; (B) size distribution of Cu-NPs, with measurements obtained from the TEM images.

doi:10.1371/journal.pone.0149484.g001

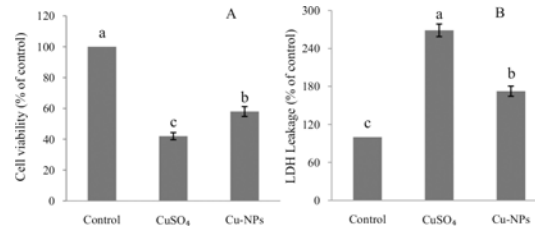


**Fig 2. Cell viability and lactate dehydrogenase (LDH) leakage in primary hepatocytes of juvenile *E. coioides* after CuSO<sub>4</sub> or Cu-NPs exposure.** Data are means ±SD (n = 3). Significant differences ( $p < 0.05$ ) among treatments were indicated by different letters.

doi:10.1371/journal.pone.0149484.g002

with CuSO<sub>4</sub> resulting in significantly higher ROS than the equal concentration of Cu-NPs ( $p < 0.05$ ).

### Oxidative stress in hepatocytes

The changes in lipid peroxidation and antioxidant capacity are shown in Fig (3B–3E). Compared to control, either CuSO<sub>4</sub> or Cu-NPs caused a significant increase in MDA formation ( $p < 0.05$ ), and significant decreases in the activities of T-SOD, CAT and GSH ( $p < 0.05$ ), more so in the CuSO<sub>4</sub> than Cu-NPs treatment.

### Cell apoptosis and necrosis

The percent of apoptotic (Fig 4A) and necrotic hepatocytes (Fig 4B) was significantly higher after the CuSO<sub>4</sub> or Cu-NPs treatment compared with the control ( $p < 0.05$ ), with CuSO<sub>4</sub>

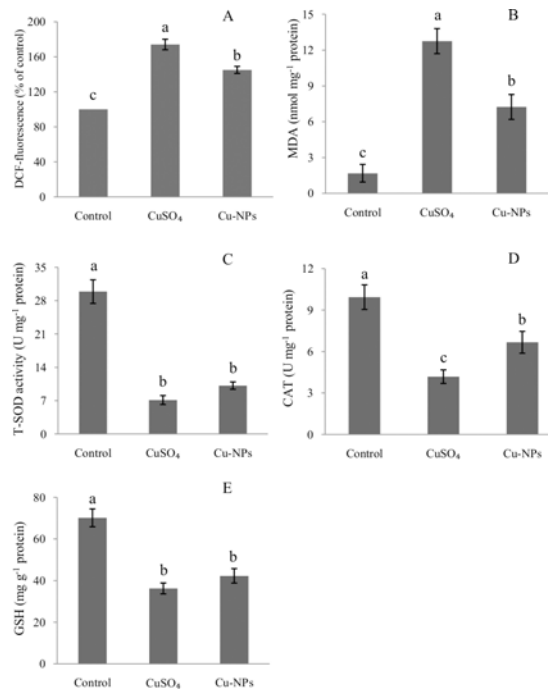


**Fig 3. Reactive oxygen species (ROS) formation (A) and oxidative stress (B-E) in the primary hepatocytes of juvenile *E. coioides* after CuSO<sub>4</sub> or Cu-NPs exposure.** Data are means ±SD (n = 3). Significant differences ( $p < 0.05$ ) among treatments were indicated by different letters.

doi:10.1371/journal.pone.0149484.g003

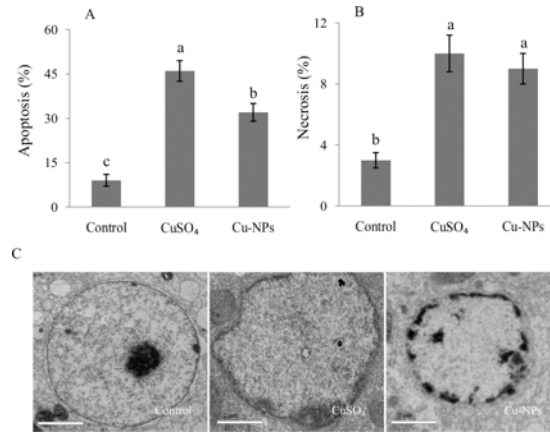


**Fig 4. Cell apoptosis and necrosis in the primary hepatocytes of juvenile *E. coioides* after CuSO<sub>4</sub> or Cu-NPs exposure.** (A) cell apoptosis; (B) cell necrosis; (C) the nuclear ultrastructure examined by transmission electron microscopy (TEM), scale bar = 2 μm. Data are means ±SD (n = 3). Significant differences ( $p < 0.05$ ) among treatments were indicated by different letters.

doi:10.1371/journal.pone.0149484.g004

causing higher apoptosis and necrosis than Cu-NPs. The ultrastructural alterations in apoptotic cells were observed under transmission electron microscopy (Fig 4C). The control cells displayed normal nuclear morphology. In contrast, either CuSO<sub>4</sub> or Cu-NPs treatment resulted in typical apoptotic features including chromatin condensation and margination at the nuclear periphery.

### Cytochrome c

Compared to control, exposure to either CuSO<sub>4</sub> or Cu-NPs induced a significant increase in cytochrome c concentrations in the cytosol and a significant decrease in mitochondria ( $p < 0.05$ ) (Fig 5), more so in the CuSO<sub>4</sub> than Cu-NPs treatment.

### Caspase activities

Apoptosis was evaluated by proteolytic activities of caspase-3, caspase-8 and caspase-9 (Fig 6). After CuSO<sub>4</sub> or Cu-NPs exposure, significant increases in caspase-3, caspase-8 and caspase-9 activities were noticed compared to control ( $p < 0.05$ ), with the CuSO<sub>4</sub> treatment resulting in significantly higher caspase-3, caspase-8 and caspase-9 activities than Cu-NPs ( $p < 0.05$ ).

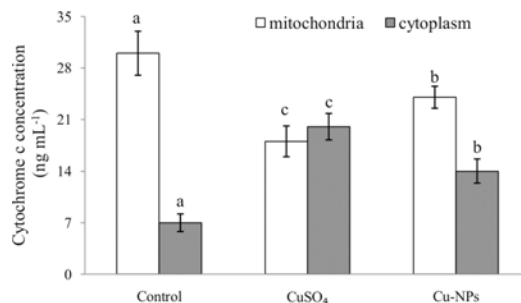


**Fig 5. Cytochrome c concentration in primary hepatocytes of juvenile *E. coioides* after CuSO<sub>4</sub> or Cu-NPs exposure.** Data are means ±SD (n = 3). Different letters denoted results significantly different from control ( $p < 0.05$ ).

doi:10.1371/journal.pone.0149484.g005



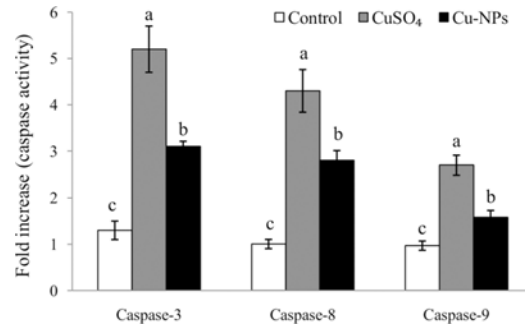


**Fig 6. Caspases activities in primary hepatocytes of juvenile *E. coioides* after CuSO<sub>4</sub> or Cu-NPs exposure.** Data are means  $\pm$ SD ( $n = 3$ ). Significant differences ( $p < 0.05$ ) among treatments were indicated by different letters.

doi:10.1371/journal.pone.0149484.g006

## Gene expression

Compared to control, the antioxidative-related genes [*SOD (Cu/Zn)*, *SOD (Mn)*, *Gpx4*, *CAT*] were significantly down-regulated. However, genes related to apoptosis (*p53*, *p38 $\beta$*  and *TNF- $\alpha$* ) were significantly up-regulated in hepatocytes than control after CuSO<sub>4</sub> or Cu-NPs treatment ( $p < 0.05$ ) (Fig 7).

## Protein abundance

Compared to control, abundance of p53 protein was increased more in the CuSO<sub>4</sub> than Cu-NPs treatment (Fig 8).

## Discussion

To our knowledge, this is the first study that focused on the effects of CuSO<sub>4</sub> or Cu-NPs on hepatocyte primary cultures of *E. coioides*. The primary and secondary nanoparticle sizes are regarded as important parameters for *in vitro* cytotoxicity in a cell culture medium [17]; therefore, the behavior of Cu-NPs in cell culture medium was evaluated through nanoparticle tracking analysis (NTA) to understand the extent of aggregation and secondary size of these nanoparticles before cellular exposure. In the present study, the average diameter of Cu-NPs in the cell culture medium was larger ( $100 \pm 35$  nm) than the primary particle diameter ( $80 \pm 32$  nm), suggesting aggregation of nanoparticles. However, the average secondary particle diameter was smaller in the cell culture medium ( $100 \pm 35$  nm) than seawater ( $210 \pm 130$  nm) in our previous study [7], suggesting relatively less particle aggregation in the cell culture medium than seawater. These results were corroborated well by other reports [17,32].

In the present study, primary *E. coioides* hepatocyte cultures were used to demonstrate CuSO<sub>4</sub> or Cu-NPs cytotoxicity as measured by the MTT and LDH assays. It is worth emphasizing that MTT assay reflects only the changes in mitochondrial function, and is not indicative of the manner or stages of cell death [24, 33]. Niska et al. [33] reported that a reduction in the amount of formazan produced from MTT can be proportional to the cell number. Cui et al. [27] reported LDH is a soluble cytosolic enzyme present in most eukaryotic cells that is released into the culture medium upon cell death due to plasma membrane damage. Hence, an increase in the LDH activity in culture supernatant is proportional to the number of lysed cells [34]. In the present study, the proportion of viable cells declined after CuSO<sub>4</sub> or Cu-NPs exposure compared to control. The question remained as to how CuSO<sub>4</sub> or Cu-NPs induced cell death.

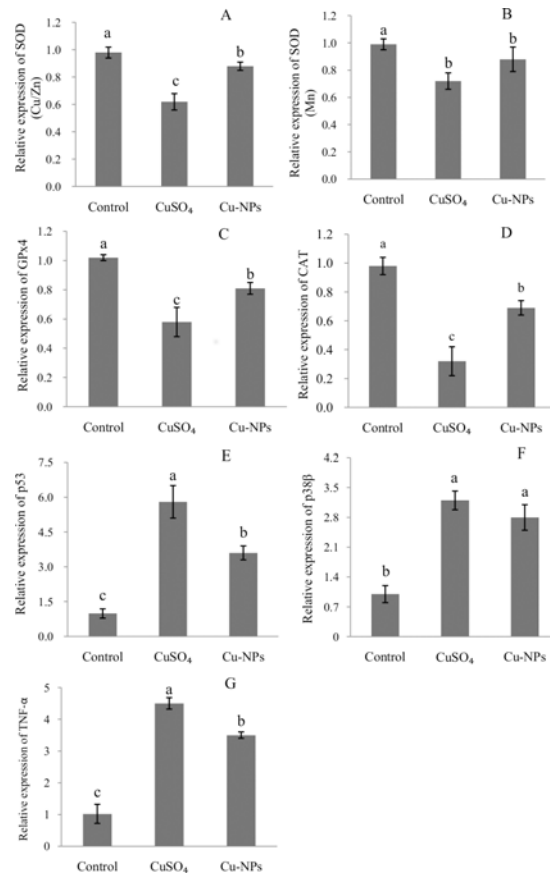


**Fig 7. Anti-oxidative and apoptosis-related gene expressions in primary hepatocytes of juvenile *E. coioides* after CuSO<sub>4</sub> or Cu-NPs exposure.** Anti-oxidative related gene expression (A-D), apoptosis related gene expression (E-G). Data are means ±SD (n = 3). Significant differences (p < 0.05) among treatments were indicated by different letters.

doi:10.1371/journal.pone.0149484.g007

Evidence of hazardous health effect of nanoparticles is increasing rapidly. ROS generation has been proposed as a possible mechanism involved in the toxicity of nanoparticles [24,35]. Valko et al. [36] and Paz-Elizur et al. [37] reported ROS are generally considered cytotoxic because the free radicals cause oxidative damage to biomolecules such as DNA, proteins and lipids through oxidative modifications. However, studies on the exact mechanisms by which nanoparticles generated ROS in cells are still underway [24]. In the present study, we found that CuSO<sub>4</sub> or Cu-NPs increased cellular ROS generation. These results are in good agreement

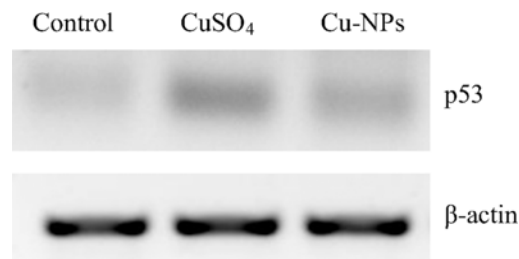


**Fig 8. p53 protein expression in primary hepatocytes of juvenile *E. coioides* after CuSO<sub>4</sub> or Cu-NPs exposure.**

doi:10.1371/journal.pone.0149484.g008

with Jia et al. [14] and Cui et al. [27]. We also observed an increase in MDA concentration (a marker of lipid peroxidation) and decreases in the activities of antioxidants including T-SOD, CAT and GSH following the CuSO<sub>4</sub> or Cu-NPs treatment. In addition, the antioxidative-related genes [*SOD (Cu/Zn)*, *SOD (Mn)*, *CAT*, *GPx4*] were also down-regulated in hepatocytes, consistent with earlier findings that CuSO<sub>4</sub> or Cu-NPs reduced T-SOD, CAT and GSH activities in whole-fish cultured in seawater [7]. Hence, we conclude that (1) toxicity to whole fish can be replicated in hepatocyte cultures; (2) Cu from CuSO<sub>4</sub> or Cu-NPs stimulated the intracellular ROS generation, altered the antioxidative enzymatic defense systems in primary hepatocytes of *E.coioides* causing apoptosis and necrosis. Our study also found higher ROS generation, higher MDA concentration, lower activities of antioxidative enzymes T-SOD and CAT and lower concentration of antioxidant GSH in the CuSO<sub>4</sub> than Cu-NPs treatment. However, Thit et al. [38] reported Cu-NPs were more toxic than soluble Cu to kidney epithelial cells from frog *Xenopus laevis* (A6). The difference between the two studies could be due to different animal species; it should also be kept in mind that differential susceptibility to Cu could exist between freshwater and seawater species.

ROS are important for apoptosis [2,14]. The mechanisms driving apoptosis in cells under oxidative stress may involve high ROS concentration directly inhibiting caspase (cysteine protease) activity, disrupting intracellular Ca<sup>2+</sup> homeostasis, and leading to ATP (adenosine triphosphate) depletion [39]. In the present study, apoptosis and necrosis in hepatocytes were significantly higher after CuSO<sub>4</sub> or Cu-NPs treatment than in control. Thus, oxidative stress likely plays an important role in apoptosis induced by CuSO<sub>4</sub> or Cu-NPs in *E.coioides* hepatic cells.

Apoptosis is a highly organized and genetically-controlled type of cell death that occurs under a variety of physiological and pathological conditions [22,40]. Although apoptosis can be triggered by various stimuli, there are two main apoptotic pathways: mitochondria-initiated intrinsic and death receptor-triggered extrinsic [41]. Both pathways activate a set of caspases [14]. In general, caspase-3 is the major operational caspase, which plays an essential role in apoptosis by mediating a subsequent lethal chain of events [22]. Caspase-8 and caspase-9 are the major initiator caspases implicated in the two pathways [42].

Many studies have demonstrated apoptosis via caspase-dependent pathway [14,18,22]. In the present study, a significant increase in the activities of caspase-3, caspase-8 and caspase-9 was noticed after CuSO<sub>4</sub> or Cu-NPs exposure compared to control, indicating that CuSO<sub>4</sub> or Cu-NPs participated in the activation of caspases to induce hepatocyte apoptosis. Our study also found the CuSO<sub>4</sub> treatment induced higher caspase-3, caspase-8 and caspase-9 activities than the Cu-NPs treatment, suggesting caspases in the primary hepatocytes of *E.coioides* were more sensitive to Cu ions than Cu-NPs.

Several signaling pathways have been implicated in the initiation of the caspase cascade. One of the most well defined pathways for pro-caspase activation is the translocation of cytochrome c from mitochondria to the cytosol [43]. The disruption of the mitochondrial membranes may allow cytochrome c leakage into the cytosol [44], with the released cytochrome c and deoxyadenosine triphosphate (dATP) binding to the apoptotic protease activating factor-1 (APAF-1), leading to the recruitment and activation of caspases [14,22]. In the present study, we investigated a key event in the activation of caspases, the release of cytochrome c, and demonstrated that apoptosis in primary hepatocytes induced by CuSO<sub>4</sub> or Cu-NPs was accompanied by enhanced release of cytochrome c into the cytoplasm. The mechanism of cytochrome c release from mitochondria is not well understood, but it may be associated with an interaction of ROS with mitochondria [45].

To clarify a possible mechanism of apoptosis, we investigated the effects of CuSO<sub>4</sub> and Cu-NPs on apoptosis-related genes and p53 protein. The tumor-suppressor protein p53 is a universal

sensor of environmental stress and, as a transcription factor, plays a critical role in regulating expression of genes involved in mediating growth arrest and/or apoptosis [30]. Ahamed et al. [24] reported p53 protein triggered a cell cycle arrest (to provide time for the damage to be repaired) or self-mediated apoptosis in the presence of DNA damage or cellular stress; consequently, p53 has been used as a sensitive biomarker in response to gene toxicity. In this study, gene expression and abundance of p53 increased in hepatocytes after CuSO<sub>4</sub> or Cu-NPs treatment, with CuSO<sub>4</sub> being more effective than the equal concentration of Cu-NPs. Those results indicated that CuSO<sub>4</sub> or Cu-NPs induced gene toxicity to primary *E.coioides* hepatocytes, and activation of p53 by genotoxic injury can result in either growth arrest or apoptosis. Qi et al. [30] found that transcription of p53 could be activated by increased ROS generation; indeed, ROS are considered a key factor in the activation of p53 by many chemotherapeutic agents and stimuli that may not be DNA-damaging agents [46]. However, further studies are needed to elucidate pathways enabling ROS to influence abundance of protein p53.

The p38 mitogen-activated protein kinases (MAPKs) (including p38a, p38b and p38β) are the signaling molecules involved in regulation of cellular responses to various extracellular stimuli [47]. Cai et al. [15] reported p38β played a crucial role in regulating apoptosis. In the present study, we found p38β was up-regulated in hepatocytes after CuSO<sub>4</sub> or Cu-NPs treatment, with CuSO<sub>4</sub> resulting in higher p38β gene expression than Cu-NPs.

TNF-α, a pleiotropic cytokine, mediates metal-induced hepatotoxicity by inflammatory signaling pathways and stimulates inflammation and fibrosis; when protein synthesis is repressed, TNF-α turns into a death factor causing cells apoptosis [14,48]. Suska et al. [48] reported oxidative stress triggered the TNF-α release, and resulted in exacerbated apoptosis. Pan et al. [49] reported overexpressing of TNF-α could cause endotoxic shock and may contribute to fish disease. In our study, the gene expression of TNF-α was significantly up-regulated in hepatocytes after CuSO<sub>4</sub> or Cu-NPs treatment compared to control, with CuSO<sub>4</sub> exposure resulting in higher TNF-α expression than the equal concentration of Cu-NPs. These findings indicated either form of Cu may contribute to primary hepatocyte pathologies and exacerbated apoptosis (as judged from flow cytometry analysis), but Cu ions may cause more severe toxicity to primary hepatocytes than Cu-NPs.

## Conclusions

The present study demonstrated the mechanisms of Cu-NPs and CuSO<sub>4</sub> toxicity to hepatocytes (Fig 9). Cu-NPs had similar types of toxic mechanisms as CuSO<sub>4</sub> on primary hepatocytes of *E. coioides*. Exposure to either Cu-NPs or CuSO<sub>4</sub> increased cellular ROS. These ROS could induce oxidative stress and lipid peroxidation, which impaired membrane structure and anti-oxidant defense system. In addition, increased ROS may impair mitochondrial bioenergetics and

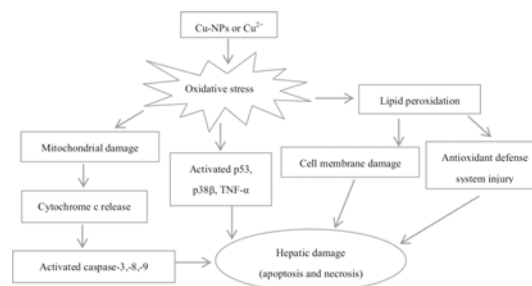


**Fig 9. Scheme showing the proposed mechanisms of Cu-NPs and CuSO<sub>4</sub> toxicity to primary hepatocytes of *E.coioides*.** Cu-NPs and CuSO<sub>4</sub> exhibited similar types of toxic mechanisms.

doi:10.1371/journal.pone.0149484.g009

physiological functions. Subsequently, a release of mitochondrial cytochrome c into the cytosol activated caspases, triggering apoptosis. In addition, the apoptosis-related genes (*p53*, *p38 $\beta$*  and *TNF- $\alpha$* ) were activated by oxidative stress. Due to their cytotoxic effects, both CuSO<sub>4</sub> and Cu-NPs should be strictly monitored in the *E.coioides* culture.

## Acknowledgments

We thank Prof. Zed Rengel from the University of Western Australia for valuable comments on the manuscript. We also express our sincere thanks to the anonymous reviewers.

## Author Contributions

Conceived and designed the experiments: XL ZL SY. Performed the experiments: TW. Analyzed the data: TW XC. Contributed reagents/materials/analysis tools: XL ZL. Wrote the paper: TW. Obtained permission for use of cell: ZL XL.

## References

1. Ju-Nam Y, Lead JR. Manufactured nanoparticles: an overview of their chemistry, interactions and potential environmental implications. *Sci Total Environ*. 2008; 400: 396–414. doi: [10.1016/j.scitotenv.2008.06.042](https://doi.org/10.1016/j.scitotenv.2008.06.042) PMID: [18715626](https://pubmed.ncbi.nlm.nih.gov/18715626/)
2. Bondarenko O, Juganson K, Ivask A, Kasemets K, Mortimer M, Kahru A. Toxicity of Ag, CuO and ZnO nanoparticles to selected environmentally relevant test organisms and mammalian cells in vitro: a critical review. *Arch Toxicol*. 2013; 87: 1181–1200. doi: [10.1007/s00204-013-1079-4](https://doi.org/10.1007/s00204-013-1079-4) PMID: [23728526](https://pubmed.ncbi.nlm.nih.gov/23728526/)
3. Moos NV, Maillard L, Slaveykova VI. Dynamics of sub-lethal effects of nano-CuO on the microalga *Chlamydomonas reinhardtii* during short-term exposure. *Aquat Toxicol*. 2015; 161: 267–275. doi: [10.1016/j.aquatox.2015.02.010](https://doi.org/10.1016/j.aquatox.2015.02.010) PMID: [25731685](https://pubmed.ncbi.nlm.nih.gov/25731685/)
4. Nowack B, Ranville JF, Diamond S, Gallego-Urrea JA, Metcalfe C, Rose J, et al. Potential scenarios for nanomaterial release and subsequent alteration in the environment. *Environ Toxicol Chem*. 2012; 31: 50–59. doi: [10.1002/etc.726](https://doi.org/10.1002/etc.726) PMID: [22038832](https://pubmed.ncbi.nlm.nih.gov/22038832/)
5. Aruoja V, Dubourguier HC, Kasemets K, Kahru A. Toxicity of nanoparticles of CuO, ZnO and TiO<sub>2</sub> to microalgae *Pseudokirchneriella subcapitata*. *Sci Total Environ*. 2009; 407: 1461–1468. doi: [10.1016/j.scitotenv.2008.10.053](https://doi.org/10.1016/j.scitotenv.2008.10.053) PMID: [19038417](https://pubmed.ncbi.nlm.nih.gov/19038417/)
6. Handy RD, Al-Bairuty G, Al-Jubory A, Ramsden CS, Boyle D, Shaw BJ, et al. Effects of manufactured nanomaterials on fishes: a target organ and body systems physiology approach. *J Fish Biol*. 2011; 79: 821–853. doi: [10.1111/j.1095-8649.2011.03080.x](https://doi.org/10.1111/j.1095-8649.2011.03080.x) PMID: [21967577](https://pubmed.ncbi.nlm.nih.gov/21967577/)
7. Wang T, Long X, Cheng Y, Liu Z, Yan S. The potential toxicity of copper nanoparticles and copper sulphate on juvenile *Epinephelus coioides*. *Aquat Toxicol*. 2014; 152: 96–104. doi: [10.1016/j.aquatox.2014.03.023](https://doi.org/10.1016/j.aquatox.2014.03.023) PMID: [24742820](https://pubmed.ncbi.nlm.nih.gov/24742820/)
8. Lin YH, Shie YY, Shiau SY. Dietary copper requirements of juvenile grouper *Epinephelus malabaricus*. *Aquaculture* 2008; 274: 161–165.
9. Liu XJ, Luo Z, Xiong BX, Liu X, Zhao YH, Hu GF, et al. Effect of waterborne copper exposure on growth, hepatic enzymatic activities and histology in *Synechogobius hasta*. *Ecotox Environ Safe*. 2010; 73: 1286–1291.
10. Al-Bairuty GA, Shaw BJ, Handy RD, Henry TB. Histopathological effects of waterborne copper nanoparticles and copper sulphate on the organs of rainbow trout (*Oncorhynchus mykiss*). *Aquat Toxicol*. 2013; 126: 104–115. doi: [10.1016/j.aquatox.2012.10.005](https://doi.org/10.1016/j.aquatox.2012.10.005) PMID: [23174144](https://pubmed.ncbi.nlm.nih.gov/23174144/)
11. Li J, Quabius ES, Bonga SEW, Flik G, Lock RAC. Effects of water-borne copper on bronchial chloride cells and Na<sup>+</sup>/K<sup>+</sup>-ATPase activities in Mozambique tilapia (*Oreochromis mossambicus*). *Aquat Toxicol*. 1998; 43: 1–11.
12. Shaw BJ, Al-Bairuty G, Handy RD. Effects of waterborne copper nanoparticles and copper sulphate on rainbow trout, (*Oncorhynchus mykiss*): Physiology and accumulation. *Aquat Toxicol*. 2012; 116–117: 90–101. doi: [10.1016/j.aquatox.2012.02.032](https://doi.org/10.1016/j.aquatox.2012.02.032) PMID: [22480992](https://pubmed.ncbi.nlm.nih.gov/22480992/)
13. Kong X, Jiang H, Wang S, Wu X, Fei W, Li L, et al. Effects of copper exposure on the hatching status and antioxidant defense at different developmental stages of embryos and larvae of goldfish *Carassius auratus*. *Chemosphere* 2013; 92: 1458–1464. doi: [10.1016/j.chemosphere.2013.04.004](https://doi.org/10.1016/j.chemosphere.2013.04.004) PMID: [23623536](https://pubmed.ncbi.nlm.nih.gov/23623536/)

14. Jia R, Cao L, Du J, Wang J, Liu Y, Jeney G, et al. Effects of carbon tetrachloride on oxidative stress, inflammatory response and hepatocyte apoptosis in common carp (*Cyprinus carpio*). *AquatToxicol*. 2014; 152: 11–19.
15. Cai J, Huang Y, Wei S, Huang X, Ye F, Fu J, et al. Characterization of p38 MAPKs from orange-spotted grouper, *Epinephelus coioides* involved in SGIV infection. *Fish Shellfish Immunol*. 2011; 31: 1129–1136. doi: [10.1016/j.fsi.2011.10.004](https://doi.org/10.1016/j.fsi.2011.10.004) PMID: [22005516](https://pubmed.ncbi.nlm.nih.gov/22005516/)
16. Cruz-Lacierda ER, Lester RJG, Eusebio PS, Marcial HS, Pedrajas SAG. Occurrence and histopathogenesis of a didymozoid trematode (*Gonapodasmius epinepheli*) in pond-reared orange-spotted grouper, *Epinephelus coioides*. *Aquaculture* 2001; 201: 211–217.
17. Saquib Q, Al-Khedhairy AA, Siddiqui MA, Abou-Tarboush FM, Azam A, Musarrat J. Titanium dioxide nanoparticles induced cytotoxicity, oxidative stress and DNA damage in human amnion epithelial (WISH) cells. *Toxicol In Vitro* 2012; 26: 351–361. doi: [10.1016/j.tiv.2011.12.011](https://doi.org/10.1016/j.tiv.2011.12.011) PMID: [22210200](https://pubmed.ncbi.nlm.nih.gov/22210200/)
18. Wang T, Long X, Liu Z, Cheng Y, Yan S. Effect of copper nanoparticles and copper sulphate on oxidation stress, cell apoptosis and immune responses in the intestines of juvenile *Epinephelus coioides*. *Fish shellfish Immunol*. 2015; 44: 674–682. doi: [10.1016/j.fsi.2015.03.030](https://doi.org/10.1016/j.fsi.2015.03.030) PMID: [25839971](https://pubmed.ncbi.nlm.nih.gov/25839971/)
19. Gomes T, Pinheiro JP, Cancio I, Pereira CG, Cardoso C, Bebianno MJ. Effects of copper nanoparticles exposure in the mussel *Mytilus galloprovincialis*. *Environ Sci Technol*. 2011; 45: 9356–9362. doi: [10.1021/es200955s](https://doi.org/10.1021/es200955s) PMID: [21950553](https://pubmed.ncbi.nlm.nih.gov/21950553/)
20. Zhao J, Wang Z, Liu X, Xie X, Zhang K, Xing B. Distribution of CuO nanoparticles in juvenile carp (*Cyprinus carpio*) and their potential toxicity. *J Hazard Mater*. 2011; 197: 304–310. doi: [10.1016/j.jhazmat.2011.09.094](https://doi.org/10.1016/j.jhazmat.2011.09.094) PMID: [22014442](https://pubmed.ncbi.nlm.nih.gov/22014442/)
21. Sovová T, Boyle D, Sloman KA, Pérez CV, Handy RH. Impaired behavioural response to alarm substance in rainbow trout exposed to copper nanoparticles. *Aquat Toxicol*. 2014; 152: 195–204. doi: [10.1016/j.aquatox.2014.04.003](https://doi.org/10.1016/j.aquatox.2014.04.003) PMID: [24792150](https://pubmed.ncbi.nlm.nih.gov/24792150/)
22. Xu WN, Liu WB, Liu ZP. Trichlorfon-induced apoptosis in hepatocyte primary cultures of *Carassius auratus gibelio*. *Chemosphere* 2009; 77: 895–901. doi: [10.1016/j.chemosphere.2009.08.043](https://doi.org/10.1016/j.chemosphere.2009.08.043) PMID: [19775726](https://pubmed.ncbi.nlm.nih.gov/19775726/)
23. Shaw BJ, Handy RD. Physiological effects of nanoparticles on fish: a comparison of nanometals versus metal ions. *Environ Int*. 2011; 37: 1083–1097. doi: [10.1016/j.envint.2011.03.009](https://doi.org/10.1016/j.envint.2011.03.009) PMID: [21474182](https://pubmed.ncbi.nlm.nih.gov/21474182/)
24. Ahamed M, Siddiqui MA, Akhtar MJ, Ahmad I, Pant AB, Alhadlaq HA. Genotoxic potential of copper oxide nanoparticles in human lung epithelial cells. *Biochem Biophys Res Commun*. 2010; 396: 578–583. doi: [10.1016/j.bbrc.2010.04.156](https://doi.org/10.1016/j.bbrc.2010.04.156) PMID: [20447378](https://pubmed.ncbi.nlm.nih.gov/20447378/)
25. Rocchetta I, Mazzuca M, Conforti V, Ruiz L, Balzaretto V, de Molina MDR. Effect of chromium on the fatty acid composition of two strains of *Euglena gracilis*. *Environ Pollut*. 2006; 141: 353–358. PMID: [16213072](https://pubmed.ncbi.nlm.nih.gov/16213072/)
26. Bradford M. A rapid and sensitive method for the quantitation of microgram quantities of protein utilizing the principle of protein-dye binding. *Anal Biochem*. 1976; 72: 248–254. PMID: [942051](https://pubmed.ncbi.nlm.nih.gov/942051/)
27. Cui Y, Liu B, Xie J, Xu P, Habte-Tsion HM, Zhang Y. The effect of emodin on cytotoxicity, apoptosis and antioxidant capacity in the hepatic cells of grass carp (*Ctenopharyngodon idellus*). *Fish Shellfish Immunol*. 2014; 38: 74–79. doi: [10.1016/j.fsi.2014.02.018](https://doi.org/10.1016/j.fsi.2014.02.018) PMID: [24631735](https://pubmed.ncbi.nlm.nih.gov/24631735/)
28. Telford WG, King LE, Fraker PJ. Evaluation of glucocorticoid-induced DNA fragmentation in mouse thymocytes by flow cytometry. *Cell Prolif*. 1991; 24: 447–459. PMID: [1657218](https://pubmed.ncbi.nlm.nih.gov/1657218/)
29. Dan XM, Zhang TW, Li YW, Li AX. Immune responses and immune-related gene expression profile in orange-spotted grouper after immunization with *Cryptocaryon irritans* vaccine. *Fish Shellfish Immunol*. 2013; 34: 885–891. doi: [10.1016/j.fsi.2012.12.011](https://doi.org/10.1016/j.fsi.2012.12.011) PMID: [23291105](https://pubmed.ncbi.nlm.nih.gov/23291105/)
30. Qi ZH, Liu YF, Luo SW, Chen CX, Liu Y, Wang WN. Molecular cloning, characterization and expression analysis of tumor suppressor protein p53 from orange-spotted grouper, *Epinephelus coioides* in response to temperature stress. *Fish shellfish Immunol*. 2013; 35: 1466–1476. doi: [10.1016/j.fsi.2013.08.011](https://doi.org/10.1016/j.fsi.2013.08.011) PMID: [24012751](https://pubmed.ncbi.nlm.nih.gov/24012751/)
31. Vera LM, Migaud H. Continuous high light intensity can induce retinal degeneration in Atlantic salmon, Atlantic cod and European sea bass. *Aquaculture* 2009; 296: 150–158.
32. Singh S, Shi T, Duffin R, Albrecht C, Berlo DV, Höhr D, et al. Endocytosis, oxidative stress and IL-8 expression in human lung epithelial cells upon treatment with fine and ultrafine TiO<sub>2</sub>: Role of the specific surface area and of surface methylation of the particles. *Toxicol Appl Pharmacol*. 2007; 222: 141–151. PMID: [17599375](https://pubmed.ncbi.nlm.nih.gov/17599375/)
33. Niska K, Santos-Martinez MJ, Radomski MW, Inkielewicz-Stepniak I. CuO nanoparticles induce apoptosis by impairing the antioxidant defense and detoxification systems in the mouse hippocampal HT22 cell line: Protective effect of crocetin. *Toxicol In Vitro* 2015; 29: 663–671. doi: [10.1016/j.tiv.2015.02.004](https://doi.org/10.1016/j.tiv.2015.02.004) PMID: [25701151](https://pubmed.ncbi.nlm.nih.gov/25701151/)

34. Selvaraj V, Armistead MY, Cohenford M, Murray E. Arsenic trioxide (As<sub>2</sub>O<sub>3</sub>) induces apoptosis and necrosis mediated cell death through mitochondrial membrane potential damage and elevated production of reactive oxygen species in PLHC-1 fish cell line. *Chemosphere* 2013; 90: 1201–1209. doi: [10.1016/j.chemosphere.2012.09.039](https://doi.org/10.1016/j.chemosphere.2012.09.039) PMID: [23121984](https://pubmed.ncbi.nlm.nih.gov/23121984/)
35. Barillet S, Jugan ML, Laye M, Leconte Y, Herlin-Boime N, Reynaud C, et al. In vitro evaluation of SiC nanoparticles impact on A549 pulmonary cells: cyto-, genotoxicity and oxidative stress. *Toxicol Lett.* 2010; 198: 324–330. doi: [10.1016/j.toxlet.2010.07.009](https://doi.org/10.1016/j.toxlet.2010.07.009) PMID: [20655996](https://pubmed.ncbi.nlm.nih.gov/20655996/)
36. Valko M, Leibfritz D, Moncol J, Cronin M, Mazur M, Telser J. Free radicals and antioxidants in normal physiological functions and human disease. *Int J Biochem Cell Biol.* 2007; 39: 44–84. PMID: [16978905](https://pubmed.ncbi.nlm.nih.gov/16978905/)
37. Paz-Elizur T, Sevilya Z, Leitner-Dagan Y, Elinger D, Roisman LC, Livneh Z. DNA repair of oxidative DNA damage in human carcinogenesis: potential application for cancer risk assessment and prevention. *Cancer Lett.* 2008; 266: 60–72. doi: [10.1016/j.canlet.2008.02.032](https://doi.org/10.1016/j.canlet.2008.02.032) PMID: [18374480](https://pubmed.ncbi.nlm.nih.gov/18374480/)
38. Thit A, Selck H, Bjerregaard HF. Toxic mechanisms of copper oxide nanoparticles in epithelial kidney cells. *Toxicol In Vitro.* 2015; 29: 1053–1059. doi: [10.1016/j.tiv.2015.03.020](https://doi.org/10.1016/j.tiv.2015.03.020) PMID: [25862124](https://pubmed.ncbi.nlm.nih.gov/25862124/)
39. McConkey DJ. Biochemical determinants of apoptosis and necrosis. *Toxicol Lett.* 1998; 99: 157–168. PMID: [9862281](https://pubmed.ncbi.nlm.nih.gov/9862281/)
40. Guicciardi M, Gores G. Apoptosis: a mechanism of acute and chronic liver injury. *Gut* 2005; 54: 1024–1033. PMID: [15951554](https://pubmed.ncbi.nlm.nih.gov/15951554/)
41. Kumar S. Caspase function in programmed cell death. *Cell Death Differ.* 2007; 14: 32–43. PMID: [17082813](https://pubmed.ncbi.nlm.nih.gov/17082813/)
42. Larsen BD, Rampalli S, Burns LE, Brunette S, Dilworth FJ, Megeney LA. Caspase 3/caspase-activated DNase promote cell differentiation by inducing DNA strand breaks. *Proc Natl Acad Sci USA* 2010; 107: 4230–4235. doi: [10.1073/pnas.0913089107](https://doi.org/10.1073/pnas.0913089107) PMID: [20160104](https://pubmed.ncbi.nlm.nih.gov/20160104/)
43. DaMata JP, Mendes BP, Maciel-Lima K, Alves C, Menezes S, Dutra WO, et al. Distinct macrophage fates after *in vitro* infection with different species of *Leishmania*: induction of apoptosis by *Leishmania (Leishmania) amazonensis*, but not by *Leishmania (Viannia) guyanensis*. *PLoS ONE* 2015; 10 (10): e0141196. doi: [10.1371/journal.pone.0141196](https://doi.org/10.1371/journal.pone.0141196) PMID: [26513474](https://pubmed.ncbi.nlm.nih.gov/26513474/)
44. Chang CC, Lee PP, Liu CH, Cheng W. Trichlorfon, an organophosphorus insecticide, depresses the immune responses and resistance to *Lactococcus garvieae* of the giant freshwater prawn *Macrobrachium rosenbergii*. *Fish Shellfish Immunol.* 2006; 20: 574–585. PMID: [16219476](https://pubmed.ncbi.nlm.nih.gov/16219476/)
45. Zhang YM, Bhavnani BR. Glutamate-induced apoptosis in primary cortical neurons is inhibited by equine estrogens via down-regulation of caspase-3 and prevention of mitochondrial cytochrome c release. *BMC Neurosci.* 2005; 6: 13–17. PMID: [15730564](https://pubmed.ncbi.nlm.nih.gov/15730564/)
46. Choi YJ, Choi JS, Jeong YJ, Lee MK, Kwon HM, Kang YH. Cellular response of flavonoids to oxidative stress: signaling for survival. *Faseb J.* 2004; 18: A906.
47. Ivanov VN, Ronai Z. p38 protects human melanoma cells from UV-induced apoptosis through down-regulation of NF-kappaB activity and Fas expression. *Oncogene* 2000; 19: 3003–3012. PMID: [10871852](https://pubmed.ncbi.nlm.nih.gov/10871852/)
48. Suska F, Esposito M, Gretzer C, Källtorp M, Tengvall P, Thomsen P. IL-1a, IL-1β and TNF-a secretion during *in vivo/ex vivo* cellular interactions with titanium and copper. *Biomaterials* 2003; 24: 461–468. PMID: [12423601](https://pubmed.ncbi.nlm.nih.gov/12423601/)
49. Pan CY, Huang TC, Wang YD, Yeh YC, Hui CF, Chen JY. Oral administration of recombinant epinecidin-1 protected grouper (*Epinephelus coioides*) and zebrafish (*Danio rerio*) from *Vibrio vulnificus* infection and enhanced immune-related gene expressions. *Fish Shellfish Immunol.* 2012; 32: 947–957. doi: [10.1016/j.fsi.2012.01.023](https://doi.org/10.1016/j.fsi.2012.01.023) PMID: [22554570](https://pubmed.ncbi.nlm.nih.gov/22554570/)